RESILIENT INFRASTRUCTURE

June 1–4, 2016

STRUCTURAL BEHAVIOUR OF REINFORCED HIGH PERFORMANCE CONCRETE COLUMNS SUBJECTED TO MONOTONIC AXIAL LOADNG

A. E. Yeganeh,
Ryerson University, Canada

K. M. A. Hossain
Ryerson University, Canada

M. S. Anwar
Ryerson University, Canada

ABSTRACT

This paper presents the results of experimental and analytical investigations on the structural performance of high performance reinforced concrete (HPC) columns subjected to monotonic axial loading. Reinforced columns made of self-consolidating concrete (SCC), engineered cementitious composite (ECC) and ultra-high performance concrete (UHPC) were tested to failure under axial loading. The test variables included concrete strength and length/slenderness of columns (classified as short and long columns). The UHPC and ECC columns demonstrated excellent ductility and higher energy absorbing capacity compared to their SCC counterparts. UHPC columns also illustrated higher ultimate load capacity compared to both ECC and SCC columns. The efficiency of UHPC and ECC columns was also judged based on strength and ductility ratio compared to their SCC counterparts. Existing models and other Code based equations were used to predict the axial load capacity as a part of analytical investigation. The predictions suggested the need for the modification of existing models/Code based equations for UHPC and ECC columns.

1. INTRODUCTION

Civil infrastructure constitutes a major proportion of Canada's wealth and thus, it behooves the scientific community and relevant industries to develop new, cost-effective construction materials with superior qualities that exceed the performance of currently available materials. During the last decades, tremendous progress has been made on the high performance concretes (HPCs). Such HPC technology involves the family of highly durable fiber reinforced engineered cementitious composite (ECC) and ultra-high strength/performance concrete (UHSC/UHPC).

Compared to traditional concrete, UHPC demonstrated advantages such as outstanding mechanical properties, ductility and durability (Acker and Behloul 2004, Hossain et al. 2011, Hossain et al. 2014; Mak et al. 2011). UHPC's higher compressive strength, improved toughness and increased damage tolerance and high strain capacity made these materials very attractive to use in heavily loaded components and civil infrastructures (Tawfik et al, 2014, Blais and Couture 1999, Hajar et al. 2004, Bierwagen and Abu-Hawash 2005, Hossain et al. 2012).

UHPC is characterized by high strength with moderate ductility while ECC materials commonly have high ductility, tight crack width and low to high strength. Poly-vinyl alcohol (PVA) fiber successfully used in the production of moderate strength ECC. ECC shows strain hardening behavior after the first crack, and demonstrates a strain capacity 300 to 500 times greater than conventional concrete. Even at large deformation, crack widths of ECC remain less than 60 μm (Li, 2003; Li & Kanda, 1998; Fischer et al. 2002). The multiple micro-cracking behavior and high strain hardening characteristic of ECC components under tension and flexure with relatively low reinforcing fibers contents (less than 2% by volume) makes it an ideal material for structural applications (Fischer and Li, 2003; Sahmaran et al. 2010; Shahman and Li 2009; Li 1998; Li et al.2001).

This paper presents the result of experimental and analytical studies on the performance of SCC, UHPC and ECC columns under axial loading. As part of the experimental program, six columns with different lengths were constructed with three different type of materials such as SCC, ECC and UHPC. The analytical study examines the axial load capacities of SCC, ECC and UHPC columns calculated based on existing standards/equations for normal and high performance concretes.

2. EXPERIMENTAL PROGRAM

2.1 Description of test specimens

As part of the experimental study, six column with three different concrete materials (SCC, ECC and UHPC) were constructed based on design as per CSA A23.3-14 standard. To study the effect of different materials on column axial load capacity, the cross section of the columns was kept constant at 160 mm x 120 mm while the heights were changed from 540 mm for short column to 1060 mm for long column. The longitudinal reinforcement consisted of 4-15M reinforcing bars ($d_b = 16mm$ and $A_s = 800mm^2$) while the transverse reinforcement consisted of 6M bars ($d_b = 6mm - bar\ diamter$ and $A_v = 60mm^2 - bar\ area$) with total of 2 legs of transverse bars in perpendicular direction of the column cross section. The detail designs for each type of columns are shown in figure1.
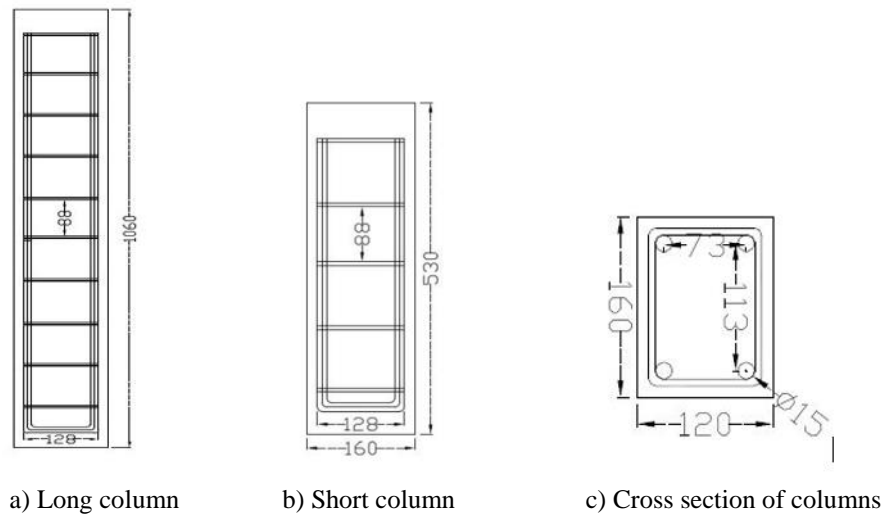

a) Long column   b) Short column   c) Cross section of columns

Figure 1: Column design details (dimensions in mm)

2.2 Material properties

The UHPC developed with water to cementitious material ratio of 0.22 and a steel fiber content of 9% by mass of dry material. It consisted of general purpose cement and silica fume as the cementing material, water, natural grain silica sand of 110 micrometer nominal size, steel fibers and a polycarboxylate-based high range water reducer. The material proportions are shown in table 1.The steel fibers used in this mix design are 0.4 mm in diameter and 14 mm in length with a tensile strength of 2160 MPa, modulus of elasticity of 210 GPa, and melting point higher than 800°C. For casting UHPC, weighted dry materials except the steel fibers were introduced to shear mixer and mixed for 2 minutes. After that again 75% of the water was added to the mixer and mixed for another 2 minutes. The remaining water and the HRWR was added gradually and mixed for another 2 minutes for the development of a uniform and consistent mix. At the end the steel fibers were added to the mix until all fibers were dispersed with mortar mixture.

The ECC mix has a water/cementitious material ratio of 0.30, PVA fiber content of 1% fibers/kg of dry material. It consists of general purpose cement and fly ash (FA) as the cementing material, water, natural grain silica sand with 110 micrometer nominal size, Polyvinyl Alcohol (PVA) fibers and a polycarboxylate-based high range water reducer (HRWR) as shown in Table1. The PVA fibers are 39 microns in diameter, 8 mm in length, a tensile strength of 1620 MPa, modulus of elasticity of 42.8 GPa, and has a melting point of 225°C. For casting ECC, weighted solid contents except for the PVA fibers were introduced into the shear mixture and mixed for 1 minutes. After that 75% of the water

was added to 50% HRWR and mixed together then the mix of water and HRWR was added gradually to the mixer and mixed for additional 2 to 3 minutes. Then the remaining water and HRWR was introduced again with same procedure to the mix, and mixed for another 2 minutes for the development of a uniform and consistent mortar mixture. Lastly, the PVA fibers were added to the mortar for another 3 minutes of stirring until all fibers were dispersed with mortar mixture. A commercial SCC mixture made of 10 mm maximum size coarse aggregates, crushed sand, Portland cement and admixtures was used.

Table 1: Mix design of UHPC and ECC

| Mixture | Ingredients per 1 part of Cement | | | | | w/b |
	Cement	Fly Ash (FA)	Silica Sand	PVA kg/m^3	HRWR kg/m^3	
UHPC	1	0.25	1.10	164	26	0.22
Mixture	Cement	Silica Fume	Silica Sand	Steel fiber kg/m^3	HRWR kg/m^3	w/b
ECC	1	1.2	0.80	26	5.4	0.27

*w: water; c: cement; b: binder

Average concrete compressive strength (f_c') obtained by testing three 100mm x 200mm concrete cylinders at 28-days, as per ASTM C39 (2003) and ASTM C109 (2011) is summarized in table 2. The four-point bending test was performed on the concrete prism specimens at 28-days according to ASTM c78 (2010). The four-point bending test was performed using a closed-loop controlled servo-hydraulic system under displacement condition at a loading rate of 0.005 mm/s. The total span length of the flexural specimens was 304.8mm. Typical load/flexural stress-mid span deflection responses of SCC/ECC/UHPC and flexural strength are presented in figure 2 and table 2, respectively. The properties of reinforcing steels were obtained based on tension test performed on three randomly selected samples for each bar size. The 15M longitudinal steel reinforcement had average yield strength (f_y) of 478 MPa and 6M transverse steel reinforcement had average yield strength of 429 MPa. Sample of stress-strain curves for steel reinforcement are shown in figure 3 with yield stress and strain values are summarized in table 3.

Table 2: Concrete compressive and flexural/tensile strength

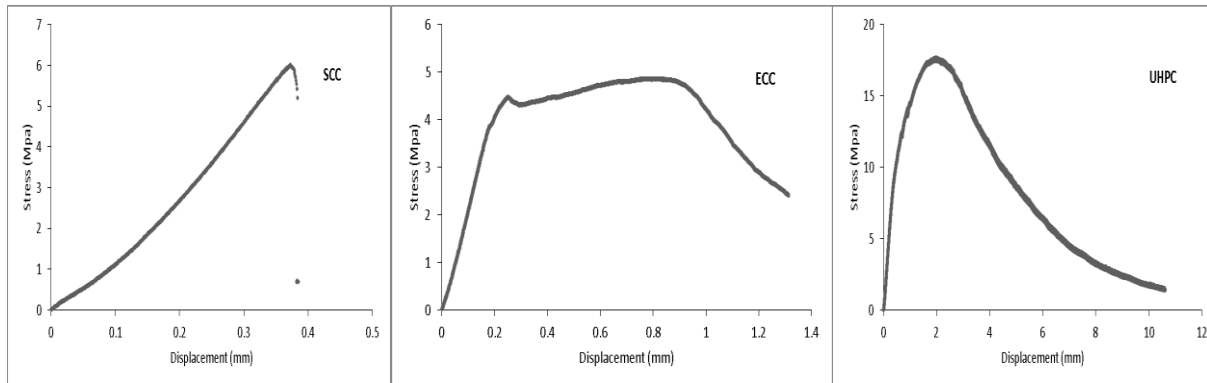|	SCC	UHPC	ECC
Concrete compressive strength (MPa) at 28 days	50.6	136	63.5
Flexural strength (MPa) at 28 days	5.9	15.7	5.1

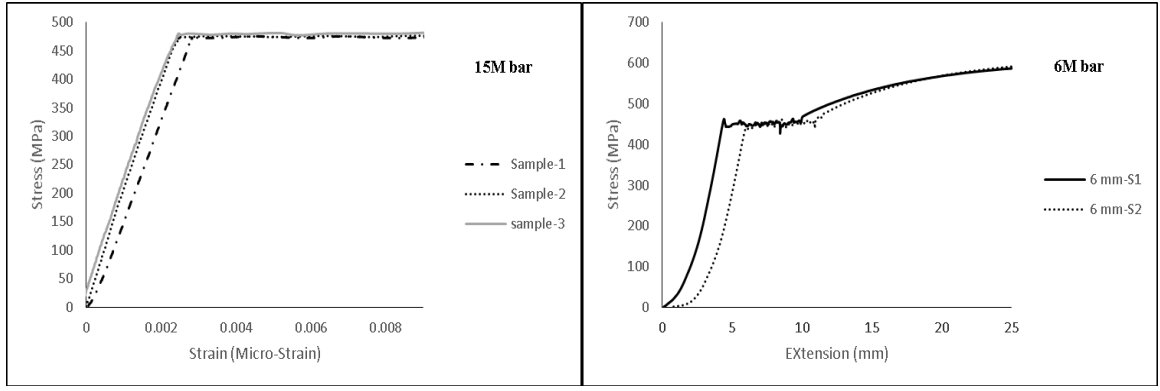Figure 2: Flexural stress-displacement responses of SCC, ECC and UHPC

Figure 3: Stress-strain/deformation responses of steel bars

Table 3: Properties of steel reinforcement

Rebar Size (mm)	Yield strain (Micro-Strain)	Yield stress (f_y) MPa
15 mm	2310	478
6 mm	**	429

2.3 Instrumentation and testing

All specimens were tested under monotonic axial loading using MTS machine. Figure 4 shows the test setup. In order to measure the horizontal displacement, one LVDT was placed in the mid-span of each sample to record the data during the loading as shown in figure 4. To measure the strain in concrete and steel reinforcement, two strain gauges were also attached - one to the surface of concrete and one to the middle of longitudinal steel reinforcement in each sample, as shown in figure 4b.


a) LVDT position   b) Steel strain gauge   c) Concrete strain gauge
Figure 4: Column test setup and LVDT/strain gauges positions

3. RESULT AND DISCUSSION

3.1 Experimental results

Figures 5a and 5b present the experimental load-vertical displacement of all long and short column specimens tested in this study, respectively. UHPC long column had more than 1100kN load capacity which was higher than short ECC and SCC columns with 900kN and 585kN load-capacity, respectively. Short UHPC column showed 100% and 200% increase in axial load-capacity compared to ECC and SCC short columns, respectively. UHPC column showed higher vertical displacement compared to its ECC and SCC counterparts by 60% and 100%, respectively.
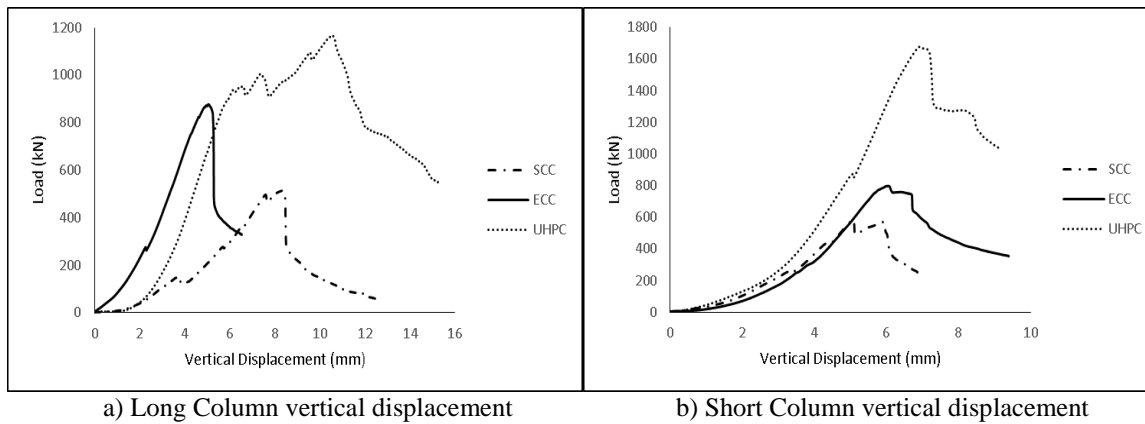
a) Long Column vertical displacement   b) Short Column vertical displacement

Figure 5: Axial load- displacement responses of SCC, ECC and UHPC columns
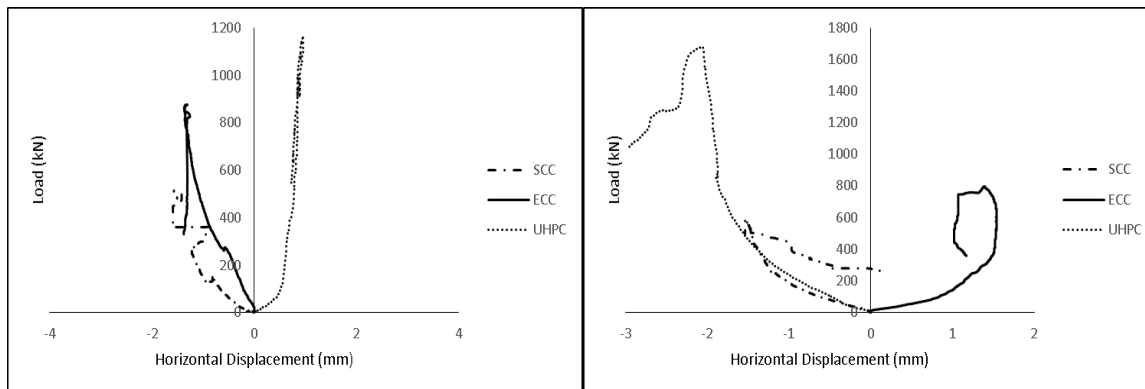
a) Long Column horizontal displacement   b) Short Column horizontal displacement

Figure 6: SCC/ECC and UHPC columns - load-horizontal/lateral displacement responses

Figures 6a and 6b compare the load-horizontal/lateral displacement responses of columns. The horizontal displacement was recorded with a LVDT positioned in the middle of the column height shown in figure 4a. All tested samples indicated a very low lateral deflection at mid-height of columns; the highest value obtained was 3 mm. None of the tested columns failed due to buckling.

Comparative load-strain responses of concrete and longitudinal steel reinforcement for long and short columns are presented in figure 7. Strains were recorded with two strain gauges attached at the mid-height of the column on concrete surface and to the longitudinal steel reinforcement as shown in figures 4b and 4c.
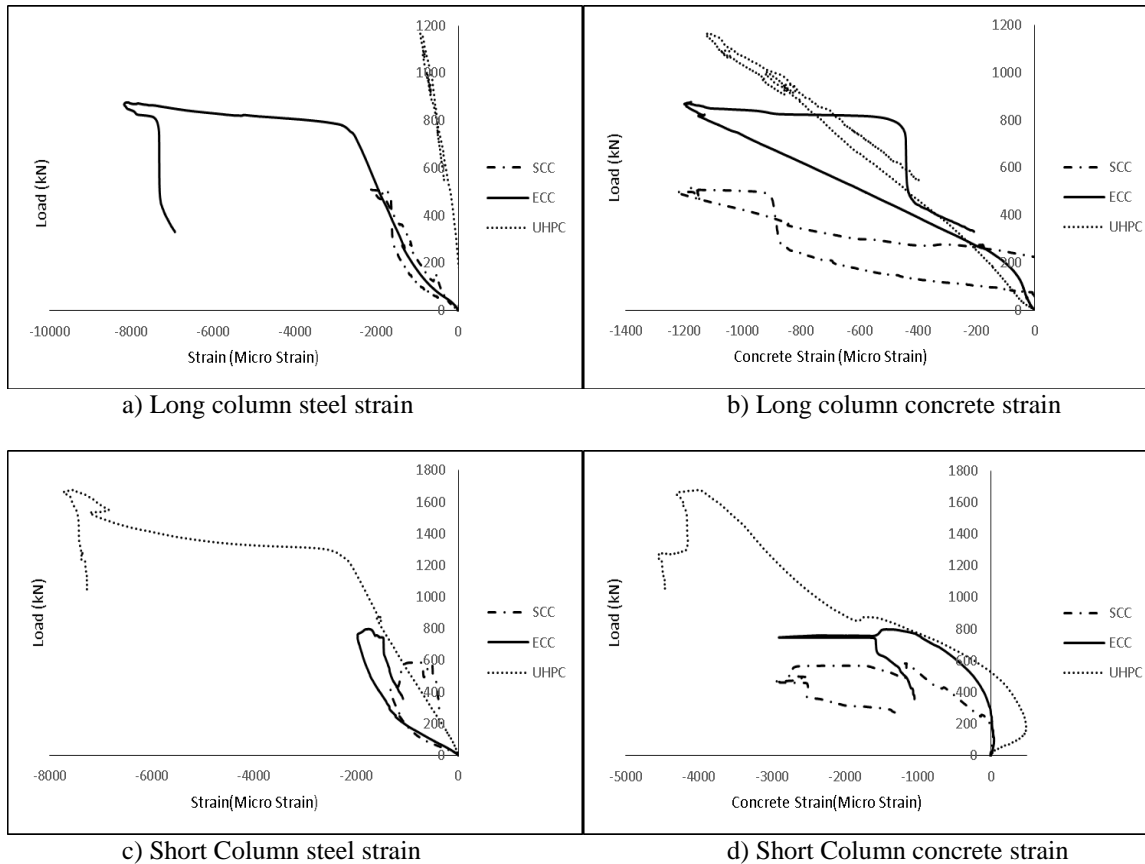
a) Long column steel strain   b) Long column concrete strain

c) Short Column steel strain   d) Short Column concrete strain

Figure 7: comparative concrete and longitudinal steel reinforcement's strains of SCC/ECC and UHPC columns
Longitudinal reinforcement for both short and long ECC columns were yielded as shown in figures 7a and 7c. Summary of axial load-capacity, vertical and horizontal displacement, concrete and steel reinforcement strains are presented in table 4.

Table 4: Summery of load-displacement and strain developments

Column Type	Concrete Type	Maximum Axial Load (kN)	Maximum Vertical Displacement (mm)	Maximum Horizontal Displacement (mm)	Concrete Strain (Micro Strain)	Steel Strain (Micro Strain)
Long Column	SCC	515.19	12.64	1.59	1228	yielded
	ECC	876.81	6.53	1.38	1199	yielded
	UHPC	1165.25	15.29	0.96	1123	1124
Short Column	SCC	584.63	6.87	1.54	2971	1327
	ECC	797.91	9.39	1.54	2903	yielded
	UHPC	1678.1	9.12	2.95	4556	yielded

The displacement ductility index (DI) for different column types and materials defined by the ratio of the displacement at 80% of ultimate load in post-peak descending part of the load-displacement curve to yield displacement at 80% of ultimate load pre-peak ascending part of the curve. Both ECC and UHPC- short and long column had shown higher ductility compared to their SCC counterparts. The summery of the ductility index for each column and the comparison between ECC/UHPC columns to their SCC counterparts are presented in table 5.

Table 5: ductility of long and short columns

Column Type	Concrete Type	Ductility Index (DI)	Ductility ratio with respect to SCC column
Long Column	SCC	1.21	1
	ECC	1.30	1.065
	UHPC	1.42	1.168
Short Column	SCC	1.24	1
	ECC	1.28	1.036
	UHPC	1.26	1.017

Comparison of failure modes of different columns exhibited that SCC columns (both short and long) failed due to severe concrete spalling at the top and bottom. However, ECC and UHPC long and short columns had shown multiple cracking development with ECC columns showing more multiple micro cracking as shown in figure 8. Localized failure of SCC columns at the top and bottom indicated that SCC columns failed to distribute the load to whole column length while ECC/UHPC columns were able to distribute the load. This can be attributed to the better confining capacity of the ECC and UHPC columns mainly due to the presence of fiber.

Figure 8: Crack patterns for ECC and UHPC columns under axial loading

3.2 Analytical studies

The axial load capacity of columns was calculated by using Codes and existing equations. The axial load capacity of SCC and ECC columns was calculated based on equation 5 as per CSA Standard A23.3-04 standard (CSA 2010). However, equation 5 based on CSA A23.3-04 has limitations for concrete compressive strength$f_c' \leq 80\ MPa$. Therefore, the UHPC column axial load capacity was calculated based on equations 1 to 4 as per Hossain (2014). Results of axial load calculations for columns are summarized in table 6.

The axial load bearing capacity (N_{Rd}) of centrically loaded UHPC-column can be determined from concrete (N_{cd}) and steel (N_{sd}) contributions according to the following equations:

[1] $N_{Rd} = N_{cd} + N_{sd}$

[2] $N_{Rd} = f_{cd}.\left(A_g - A_s\right) + f_y.A_s$

WhereA_g: concrete gross cross section;A_s: longitudinal reinforcement cross-section and f_{cd} can be obtained from equation 3.

[3] $f_{cd} = \frac{0.85 \cdot f_{ck}}{\gamma_c \cdot \gamma_c'}$

f_{ck}: Characteristic concrete compression strength, actual compressive strength resulted from experimental test. The safety factor γ_c is chosen 1.5 for in-situ concrete members and

[4] $\gamma_c' = \frac{1}{(1.1 - \frac{f_{ck}}{500})}$

As per CSA Standard A23.3-04 standard, the maximum axial load resistance of compression members is determined from equation 5:

[5] $P_{ro} = \alpha_1 \varphi_c f_c'(A_g - A_s) + \varphi_s f_y A_s$

Where P_{ro} is the axial load resistance at zero eccentricity; α_1 is the concrete stress block factor; φ_c is the resistance factor for concrete and φ_s is the resistance factor reinforcing bars. Values for φ_c and φ_s are considered equal to 1.

Table 6: Columns analytical axial load capacity

Column Type	Concrete Type	Axial Load capacity from CSA 2004 (kN)	Axial Load capacity from Hossain (kN)
Long Column	SCC	1092	------
	ECC	1252	------
	UHPC	------	1556.4
Short Column	SCC	749	------
	ECC	1252	------
	UHPC	------	1556.4

3.3 Comparison of analytical and experimental results

Analytical and experimental axial load capacities of columns are presented in table 7. Analytical load capacities of ECC and UHPC columns were higher compared to those obtained from experiments for all columns except UHPC short columns. No definite conclusions can be drawn on the prediction performance of Code/existing equations. However, the UHPC short column axial capacity seemed to be predicted reasonably by the existing equation. The lower axial load capacity of SCC columns compared to that predicted by equation can be associated with the unexpected baring failure associated with localized stress concentration at the loading points. However, more tests should be conducted to study the performance of existing equations or modify the equations for better prediction of ECC/UHPC columns.

Table 7: Analytical and experimental axial load capacities of columns

Column Type	Concrete Type	Analytical Axial Load capacity (kN)	Experimental Axial Load capacity (kN)	Ratio of experimental axial load to analytical axial load
Long Column	SCC	1092	515	0.48
	ECC	1252	877	0.7
	UHPC	1556	1165	0.75
Short Column	SCC	749	584	0.78
	ECC	1252	798	0.64
	UHPC	1556	1678	1.08

4. CONCLUSIONS

The following conclusions are drawn from experimental and theoretical analyses:

1. Both ECC and UHPC long and short columns had higher axial load capacity compared to SCC columns. Maximum axial load capacity of UHPC columns was 3 times higher (for short column) and 2 times higher (for long column) compared to their to SCC counterparts. Columns made of ECC showed increased axial load capacity compared to SCC columns - 36% higher for short columns and 70% for long columns.
2. UHPC and ECC long and short columns had exhibited higher axial displacement compared to their SCC counterparts and hence showed better ductility characteristics. Lateral/horizontal displacement of all tested columns was negligible exhibiting no buckling failure.
3. Both ECC and UHPC columns exhibited multiple crack formation all over the concrete columns. ECC columns exhibited more multiple micro-cracking behavior with tight crack width compared to UHPC/SCC columns. UHPC and ECC columns showed better load distribution capabilities through confinement effect of fiber compared to SCC columns which failed due to sever concrete spalling/bearing at the loading points.
4. No definite conclusions can be drawn on the ability of theoretical/code based equations in predicting axial load capacity of ECC/UHPC columns although predicted axial load for UHPC short columns (by existing UHPC column equation) was close to experimental value. More experimental tests are needed to develop new or modify existing equations to predict axial strength of ECC/UHPC columns.

REFRENCES

Acker, P., and Behloul, M. (2004), Ductal® Technology: A Large Spectrum of Properties,-A Wide Range of Application", *Proc. of the Int. Symp. On UHPC*, Kassel, Germany, pp.11-23.

Bierwagen, D., and Abu-Hawash, A. (2005), Ultra high performance concrete highway bridge, *Proc. of the 2005 Mid-Continent Transportation Research Symposium*, Ames, Iowa, 1-14.

Blais, P., and Couture, M. (1999), Precast, prestressed pedestrian bridge – World's first reactive powder concrete structures, PCI Journal, Sept-Oct., 60-71.

CSA Standard A23.3-04. (2010). Concrete Design Handbook, 10th edition, Ontario, Canada: CSA.

Fischer, G., and Li, V. C. (2003), "Deformation Behavior of Fiber-Reinforced Polymer Reinforced Engineered cementitious Composite (ECC) Flexural Members under Reversed Cyclic Loading Conditions", ACI Structural Jounrnal, 100(1) 25-35.

Fischer, G., and Li, V. C. (2002)," Effect of matrix ductility on deformation behavior of steel-reinforced ECC flexural members under reversed cyclic loading conditions", ACI Structural Journal, 99(6)781-790.

Hajar, Z., Lecointre, D., Simon, A., and Petitjean, J. (2004), Design and construction of the world first ultra-high performance concrete road bridges, *Proc. of the Int. Symp. On UHPC*, Kassel, Germany, September 13-15, pp.39-48.

Hossain, K.M.A., Ametrano, D., and Lachemi, M. (2014), Bond strength of GFRP bars in high strength concrete, ASCE J. of Materials in Civil Engineering, 26(3) 449-456.
Hossain, K.M.A., Ametrano, D., Mak, C., and Lachemi, M. (2011), Bond Strength and Development Length of GFRP Bars in Ultra-High Performance Concrete", Ministry of Transport Ontario (MTO) Technical Report (HIIFP Research Project), May 2011, 89p.

Hossain, K.M.A., Mak, C., and Ametrano, D. (2012), GFRP reinforced UHPC composites for sustainable bridge construction, Canadian Civil Engineer, spring (29.1) 12-15.

Hossain, K.M.A. (2014), Axial load behaviour of UHPC columns, Research report, Ryerson University, 51p.

Li, V. C. (1998), "ECC-tailored composites through micromechanical modeling", *Proceedings on the International Symposium on Fiber Reinforced Concrete: Present and the Future*, CSCE, Montreal, 64–97.

Li, V. C. (2003), "On engineered cementitious composites (ECC)–A review of the material and its applications", Advances in Concrete Technology, 1(3) 215–230.

Li, V. C. Kanda, T. (1998), "Engineered Cementitious Composites for Structural Applications" ASCE Journal, Materials in Civil Engineering, 10(2) 66-69.

Li, V. C., Wang, S., and Wu, C. (2001), "Tensile strain-hardening behavior of PVA-ECC", ACI Materials Journal, 98(6) 483–492.

Li, V. C., Wang, S., and Wu, C. (2001), "Tensile strain-hardening behavior of PVA-ECC", ACI Materials Journal, 98(6) 483–492.

Mak, C., Hossain, K.M.A., and Lachemi, M. (2011). Splice length of GFRP bars in UHPC, *2nd CSCE Int. Engineering Mechanics and Materials Specialty Conf.*, June 14-17, Ottawa.

Şahmaran, M.., Lachemi, M., Hossain, K.M.A., Ranade, R., and Li, V.C. (2010). Internal curing of ECCs for prevention of early age autogenous shrinkage cracking, Cement and Concrete Research, 39(10) 893-901.

Şahmaran, M.L., and Li, V. C. (2009), "Durability properties of micro-cracked ECC containing high volumes fly ash", Cement and Concrete Research, 39(11) 1033–1043.

Tawfik, A.S., Badr, M.R. and ElZanaty. (2014). "Behavior and ductility of high strength reinforced frames." Housing and Building National Research Center, 10, pp. 215-221.